# Mutation of I696 and W697 in the TRP box of vanilloid receptor subtype I modulates allosteric channel activation

Lucia Gregorio-Teruel,[1] Pierluigi Valente,[2] José Manuel González-Ros,[1] Gregorio Fernández-Ballester,[1] and Antonio Ferrer-Montiel[1]

[1]Instituto de Biología Molecular y Celular, Universidad Miguel Hernández, 03202 Elche, Spain
[2]Department of Experimental Medicine, Section of Physiology, University of Genova, 16132 Genova, Italy

The transient receptor potential vanilloid receptor subtype I (TRPV1) channel acts as a polymodal sensory receptor gated by chemical and physical stimuli. Like other TRP channels, TRPV1 contains in its C terminus a short, conserved domain called the TRP box, which is necessary for channel gating. Substitution of two TRP box residues—I696 and W697—with Ala markedly affects TRPV1's response to all activating stimuli, which indicates that these two residues play a crucial role in channel gating. We systematically replaced I696 and W697 with 18 native L-amino acids (excluding cysteine) and evaluated the effect on voltage- and capsaicin-dependent gating. Mutation of I696 decreased channel activation by either voltage or capsaicin; furthermore, gating was only observed with substitution of hydrophobic amino acids. Substitution of W697 with any of the 18 amino acids abolished gating in response to depolarization alone, shifting the threshold to unreachable voltages, but not capsaicin-mediated gating. Moreover, vanilloid-activated responses of W697X mutants showed voltage-dependent gating along with a strong voltage-independent component. Analysis of the data using an allosteric model of activation indicates that mutation of I696 and W697 primarily affects the allosteric coupling constants of the ligand and voltage sensors to the channel pore. Together, our findings substantiate the notion that inter- and/or intrasubunit interactions at the level of the TRP box are critical for efficient coupling of stimulus sensing and gate opening. Perturbation of these interactions markedly reduces the efficacy and potency of the activating stimuli. Furthermore, our results identify these interactions as potential sites for pharmacological intervention.

## INTRODUCTION

The transient receptor potential vanilloid type I (TRPV1) is a polymodal receptor gated by physical and chemical stimuli. This receptor is activated by noxious temperatures >42°C, and displays an outstanding temperature sensitivity, with a $Q_{10} > 20$ (Caterina and Julius, 2001; Clapham, 2003; Venkatachalam and Montell, 2007; Nilius and Owsianik, 2011). In addition, the receptor is gated by submicromolar concentrations of vanilloid compounds such as capsaicin and resiniferatoxin, and by acidic extracellular pH (Caterina and Julius, 2001). Furthermore, TRPV1 channels may be partially activated by strong depolarization (Nilius et al., 2005). Gating by this diversity of stimuli suggests the presence of multiple sensors that may work independently or in concert to activate the channel (Latorre et al., 2007; Matta and Ahern, 2007). The complexity of this multimodal gating is further complicated by its modulation through inflammation-mediated receptor phosphorylation, which notably affects the response to the activating stimuli (Premkumar and Ahern, 2000; Bhave et al., 2003; Jung et al., 2004; Mandadi et al., 2006; Pingle et al., 2007; Studer and McNaughton, 2010).

Structurally, a functional TRPV1 channel is a homotetramer of subunits assembled around a central aqueous pore (Caterina and Julius, 2001; Venkatachalam and Montell, 2007). Each subunit displays a topological organization of six transmembrane segments (S1–S6), and a cytosolic N and C terminus (Venkatachalam and Montell, 2007; Fernández-Ballester and Ferrer-Montiel, 2008). Structure–function studies aimed at identifying molecular determinants of channel gating have indicated specific domains as putative sensors of the activating stimuli (Winter et al., 2013). For instance, the capsaicin binding site has been located between the inner half of the S3–S4 segments with the contribution of other domains, and the pH sensor at the extracellular C terminus of the S5 segment (Winter et al., 2013). Similarly, the voltage sensor has been proposed to lie in the S4 and S4–S5 segments, although no clear charged residues have been identified as responsible for the charge movement necessary for gating. However, the location of the temperature sensor has been more controversial to assign, as molecular determinants have been identified in different domains of the receptor (Voets et al., 2004; Brauchi et al., 2006, 2007; Grandl et al., 2010; Yang et al., 2010; Yao et al., 2010b; Winter et al., 2013).

Correspondence to Antonio Ferrer-Montiel: aferrer@umh.es



The Rockefeller University Press $30.00
J. Gen. Physiol. Vol. 143 No. 3 361–375
www.jgp.org/cgi/doi/10.1085/jgp.201311070

In contrast, however, other studies have ascribed temperature sensing to changes in the heat capacity between the closed and open states (Clapham and Miller, 2011), or to differences in allosteric coupling between modules and the intrinsic gating of the pore (Jara-Oseguera and Islas, 2013).

The TRP domain, a 30-mer region adjacent to the channel gate, plays a pivotal role in subunit tetramerization and channel function (García-Sanz et al., 2004, 2007; Valente et al., 2008). Synthetic peptides patterned after the N terminus of this domain act as allosteric antagonists when delivered intracellularly or tethered to the plasma membrane, blocking all modes of channel gating (Valente et al., 2011). Note that a 6-mer segment in the core of the TRP domain (Fig. 1 A), referred to as the TRP box, that is highly conserved among the TRP channel family has been implicated in the allosteric coupling of stimuli sensing and pore opening. An Alanine scanning of this segment in TRPV1 identified amino acids I696 and W697 as pivotal for voltage, capsaicin, and temperature gating. Mutation of these residues to Ala significantly altered all modes of channel activation, which is consistent with a role in the allosteric mechanism of gating, rather than being part of the three sensor modules (Valente et al., 2008).

Here, we have further interrogated the role of these positions in channel function and mutated them to the 18 native L-amino acids to unveil the molecular requirements compatible with voltage and chemical gating. Notably, we found that I696 only tolerated substitutions with hydrophobic amino acids, whereas mutation of W697 to any amino acid shifted activation by voltage alone to unreachable values, although most W697X mutants were gated by capsaicin in a voltage-dependent manner. Nonetheless, the sensitivity to capsaicin activation was reduced in all mutants compared with wild type. An allosteric model of channel activation suggests that mutation of these residues primarily altered the allosteric coupling constants of the sensors to the channel gate. As a result, the free energy of channel activation was raised in the mutant channels as compared with wild-type channels. Therefore, these findings lend support to the tenet that the TRP box is a key structural element in the channel to couple the conformational changes associated with stimuli sensing to gate opening.

## MATERIALS AND METHODS

### TRPV1 receptor mutagenesis

Site-directed mutagenesis of residues I696 and W697 in the TRP box was performed in the rat TRPV1 cDNA subcloned into pcDNA3 (provided by D. Julius, Department of Physiology, University of California, San Francisco, San Francisco, CA). I696 and W697 residues were replaced with 19 of the native L-amino acids (Cys was omitted). The wild-type residues (Ile and Trp) were also introduced as an internal control, thus generating a library of 19 mutants for each position. Mutations were performed using the Pfu Turbo DNA polymerase according to the manufacturer's recommendations (QuikChange II; Agilent Technologies). A pair of degenerate primers was designed for each residue, obtaining the 19 mutants from a single PCR reaction. Mutant channels were confirmed by DNA sequencing. For mutants, the number indicates the position of the residue in the protein sequence; the first letter is the original amino acid in the wild-type protein, and the second is the residue that substitutes it. I696X and W697X denote the collection of mutants for each position.

### Cell culture and transfection

HEK293 kidney epithelial cells were cultured in DMEM GlutaMAX supplemented with 10% (vol/vol) fetal calf serum and 1% penicillin/streptomycin solution (Valente et al., 2008). Cells were grown at 37°C under 5% $CO_2$. Isolated HEK293 cells were transfected with 2 µg of DNA encoding the TRPV1 and mutant channels with Lipofectamine 2000 according to the manufacturer's recommendations (Life Technologies). Transfection efficiency for all species was ∼30%. Cells were used 48 h after transfection.

### Membrane protein biotinylation

Transfected cells (400,000) were washed twice with prechilled phosphate buffer (PBS), and incubated with 1 ml of sulfo-NHS-LC-biotin (Thermo Fisher Scientific) solution at 0.9 mg/ml diluted in PBS for 30 min at 4°C with gentle agitation. Thereafter, the reaction was quenched by adding 1 ml of Quench Biotinylation buffer in Tris-buffered saline (in mM: 10 Tris, pH 7.4, 154 NaCl) for 30 min at 4°C with agitation. Cells were scrapped-off, centrifuged, and lysed using 150 µl of RIPA buffer (in mM: 50 Hepes, pH 7.4, 140 NaCl, 10% glycerol, 1% vol/vol Triton X-100, 1 EDTA, 2 EGTA, 0.5% deoxycholate, and protease inhibitor cocktail [Sigma-Aldrich] at 1:100) at 4°C for 30 min. Protein content of cell lysates was quantified with BCA. A sample of the whole cell extract was denatured for quantitation of total channel expression. The remaining cell extract was used to affinity purify the biotinylated protein using agarose-Streptavidin (4°C, overnight) in RIPA buffer. The resin was thoroughly washed with RIPA buffer, and the bound proteins were eluted with SDS-PAGE sample buffer and denatured at 100°C for 5 min. Proteins were separated in 10% SDS-PAGE gels, electrotransferred to PVDF membranes for Western immunoblot analysis using a polyclonal anti-TRPV1 (1:30,000, rabbit; Alomone Labs) and a polyclonal anti-actin (1:10,000, rabbit; Sigma-Aldrich) overnight at 4°C. After extensive washing, membranes were exposed to anti–rabbit IgG Peroxidase conjugate (1:50,000; Sigma-Aldrich) for 1 h at room temperature while agitating and, thereafter, detected using the chemiluminescent detection reagent ECL Select (GE Healthcare). Immunoblots were digitized and quantified with TotalLab Quant software. Measurements represent mean ± SEM, $n \geq 3$.

### Patch-clamp measurements in HEK293 cells

HEK293 cells were cotransfected with TRPV1 species and the EYFP protein that was used as a reporter. Whole cell patch-clamp recordings were made as described previously (Valente et al., 2008, 2011). For electrophysiological recordings, pipette solution contained (in mM) 150 NaCl, 3 $MgCl_2$, 5 EGTA, and 10 HEPES, pH 7.2, with CsOH; and extracellular solution contained (in mM) 150 NaCl, 6 CsCl, 1 $MgCl_2$, 1.5 $CaCl_2$, 10 glucose, and 10 Hepes, pH 7.4, with NaOH. Patch pipettes were prepared from thin-walled borosilicate glass capillaries (World Precision Instruments, Inc.) and pulled with a horizontal puller (P-97; Sutter Instrument) to have a tip resistance of 3–4 MΩ once filled with internal solution. The different saline solutions were applied using a gravity-driven local microperfusion system with a rate flow of ∼200 µl/min positioned at ∼100 µm of the patched cells. All electrophysiological experiments were performed at a room temperature of 20–22°C.

Voltage step protocols consisting of 100-ms depolarizing pulses from −120 mV to 240 mV in steps of 10 mV and a repolarization to −60 mV were used. The holding potential was 0 mV. I-V relationships were studied using a ramp protocol consisting of a voltage step of 300 ms from the holding potential of 0 mV to −80 mV, followed by a 350-ms linear ramp up to 80 or 160 mV. The time interval between each step or ramp in the presence of capsaicin was 1 s, and in its absence, 10 s. Data were sampled at 10 kHz (EPC10 with Pulse software; HEKA) and low pass filtered at 3 kHz for analysis (PulseFit 8.54; HEKA). The series resistance was usually <10 MΩ, and to minimize voltage errors was compensated to 70–90%. Recordings with leak currents >100 pA or series resistance >10 MΩ were discarded.

Conductance-to-voltage (g-V) curves were obtained from the tail currents evoked by the depolarizing pulses upon repolarization to −60 mV. Normalized g-V curves were fitted to the Boltzmann equation:

$$\frac{g}{g_{max}} = P_{min} + \frac{(1 - P_{min})}{\left(1 + e^{\frac{z_g}{KT}(V - V_{0.5})}\right)},$$

where $g_{max}$ is the true maximal conductance of the channel species obtained in the presence of 100 µM capsaicin at depolarized potentials, $P_{min}$ is the minimal normalized conductance at hyperpolarized potentials ($g_{min}/g_{max}$), $V_{0.5}$ is the voltage required to activate the half-maximal conductance, and $z_g$ is the apparent gating valence. The true $g_{max}$ value was estimated from the fitting of the g-V curves in the presence of 100 µM capsaicin for the wild type and each mutant.

For voltage-dependent gating, the free energy difference between the closed and the open states at 0 mV and 22°C for a two-state model ($\Delta G_o$) was calculated using $\Delta G_o(V) = z_g F V_{0.5}$, were F is the Faraday constant (0.023 kcal/mol mV; Valente et al., 2008). For channels that display voltage-dependent and independent components in the g-V curve in the presence of capsaicin, the free energy of the activation process was obtained using $\Delta G_o = \Delta G_o(V) + \Delta G_o(I)$, where $\Delta G_o(V)$ denotes the free energy of the voltage-dependent component and $\Delta G_o(I)$ the free energy of the voltage-independent part determined (Valente et al., 2008). This energy was calculated using $\Delta G_o(I) = -RT\ \mathrm{Ln}(P_{min}/1 - P_{min})$.

### Data analysis

Data were visualized and analyzed using GraphPad Prism 5 statistical software (GraphPad Software). All data were expressed as mean ± SEM, with *n* = the number of cells tested for electrophysiological data or *n* = the number of experiments for biochemical data. Statistical analysis was performed using the Student's *t* test or the nonparametric Wilcoxon test as indicated. The $P < 0.05$ was taken as the level of significance.

## RESULTS

### Mutation of I696 and W697 notably affects voltage-activated TRPV1channel gating

A previous study identified I696 and W697 in the TRP box of TRPV1 as two pivotal molecular determinants of channel gating (Valente et al., 2008; Fig. 1 A). Mutation of both residues to Ala notably reduced the receptor response to the activating stimuli by increasing the energy of channel activation. To further investigate the role of these positions in channel gating, we mutated them to the 19 natural L-amino acids (Cys was omitted because of the reactivity of the sulfhydryl group, and Ile [in I696] and Trp [in W697] were introduced as an internal control) and evaluated the receptor phenotype in response to voltage and capsaicin. We aimed to decipher the molecular determinants compatible with channel function at these positions and to understand their pivotal role in channel gating.

Fig. 1 B displays typical voltage-evoked currents for TRPV1, mock-transfected cells, and representative I696X mutants carrying hydrophobic (I696V, I696M), aromatic (I696Y), negatively charged (I696D), polar (I696N), and positively charged (I696H) amino acids. As illustrated, mutation of position I696 to the different amino acids resulted in voltage-dependent functional channels when a hydrophobic amino acid was incorporated (Fig. 1 C). All other amino acids, with the exception of His, yielded receptors that did not respond to depolarization up to +240 mV. The responsive I696H mutant might represent the population of channels that may contain a deprotonated His, which is consistent with the observation that a charged residue in this position was not tolerated and that deprotonated His exhibits hydrophobic characteristics. This appears plausible if I696 were located in a hydrophobic environment that would decrease the $pK_a$ of His. Note that the response of functional mutants partly depends on the volume of the hydrophobic amino acid incorporated (Fig. 1 C); it is optimal for Ile, and drops when larger or smaller amino acids are incorporated.

A more significant result was obtained for W697X mutants. As shown in Fig. 1 (D and E), none of the amino acids incorporated in this position yielded voltage-sensitive channels in the range of voltages explored, not even the most conservative substitutions such as aromatic residues Tyr and Phe. Thus, mutation of W697 impacted the ability of voltage to act as a partial activator of channel gating by shifting the voltage sensitivity to unreachable voltages. This striking role of W697 in voltage sensing is intriguing because the TRP box is supposedly distant from the proposed voltage sensor. Nonetheless, it is consistent with a contribution of this domain in the downstream events that lead to gate opening upon depolarization, i.e., allosteric channel activation. Collectively, these results substantiate the notion that I696 and W697 in the TRP box are key residues transducing stimulus sensing to pore gating.

### Mutation of I696 and W697 reduced capsaicin-evoked channel gating

We next investigated the response of all mutants to capsaicin at both negative and positive membrane potentials (Fig. 2). For this purpose, we determined the current-to-voltage (I-V) relationships using a ramp protocol from −80 to 160 mV in the presence of 100 µM capsaicin. We used this saturating vanilloid concentration to ensure the response of all channels, taking into

consideration our previous results showing that mutation of these receptor sites decreased the sensitivity to the agonist (Valente et al., 2008). Fig. 2 A depicts the I-V curves of those representative I696X mutants shown in Fig. 1 B. I696X mutants incorporating a Val or Leu responded to 100 µM capsaicin to an extent similar to the response of wild-type channels or control mutation I696I to 1 µM agonist, whereas I696A, I696M, I696H, and I696F exhibited smaller current densities (Fig. 2 B). Vanilloid-induced ionic currents of I696A, I696M, and I696H mutants were much stronger at positive than at negative potentials (Fig. 2, A and B), which results in a significant current rectification at negative potentials. Incorporation of a nonhydrophobic amino acid at position I696 resulted in channels that barely responded to capsaicin at hyperpolarizing and depolarizing potentials (Fig. 2 B), in agreement with their impaired voltage sensitivity (Fig. 1, B and C), and substantiating that this site only tolerates hydrophobic amino acids for channel function.

Notwithstanding, at odds with the lack of voltage sensitivity, virtually all of the W697X mutants displayed responses to 100 µM capsaicin, independent of their physico-chemical nature (Fig. 2, C and D). A major impact is seen in large hydrophobic amino acids such as Leu, Ile, and Met, and the helical disrupting Gly and Pro. Note also that functional W697X mutants display significant ion conductance at negative and positive potentials (Fig. 2 D). These findings indicate that voltage insensitivity of most of these mutants in the absence of the vanilloid is not caused by a lack of receptor surface expression, and imply that mutation of this site may reduce voltage gating by uncoupling voltage sensing and gate opening.

### Effect of substitutions at I696 and W697 in TRPV1 channel expression

We next evaluated the impact of mutating these positions on the surface and on total protein expression. As depicted in Fig. 3 A, for the I696 position, incorporating a hydrophobic amino acid modestly affected the total expression of the protein. Similar results were obtained for nonfunctional channels incorporating other amino acids (unpublished data). Analysis of channel surface expression by protein biotinylation reveals that a lower fraction of I696A and I696M mutants are trafficked to the plasma membrane (Fig. 3 B), which is consistent with their smaller current densities.

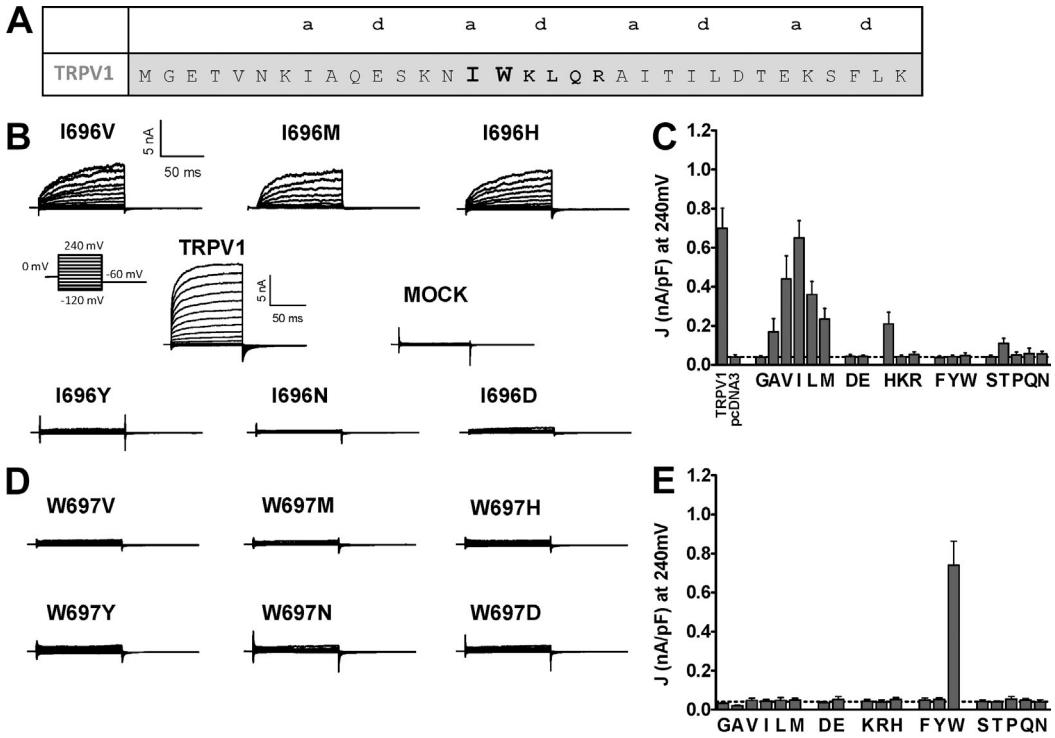


**Figure 1.** Mutation of I696 and W697 differentially affect voltage-dependent gating or TRPV1. (A) Amino acid sequence of the TRP domain of TRPV1; the residues of the TRP box are highlighted in bold, and "a" and "d" denote the positions in the predicted coiled-coil structure. (B) Family of ionic currents of representative I696X mutants, wild-type channels, and mock-transfected cells. (C) Current density at 240 mV measured for all I696X mutants using the step-voltage protocol. (D) Family of ion channel recordings evoked from representative W697X mutants. (E) Current density at 240 mV measured for all W697X mutants. The step-voltage paradigm consisted of 100-ms voltage pulses from −120 mV to 240 mV in steps of 10 mV from a holding of 0 mV and a repolarization to −60 mV (B, inset). Broken lines represent the background current density of mock-tranfected cells at 240 mV. Data are given as mean ± SEM (error bars), with $n$ (number of cells) ≥ 6.

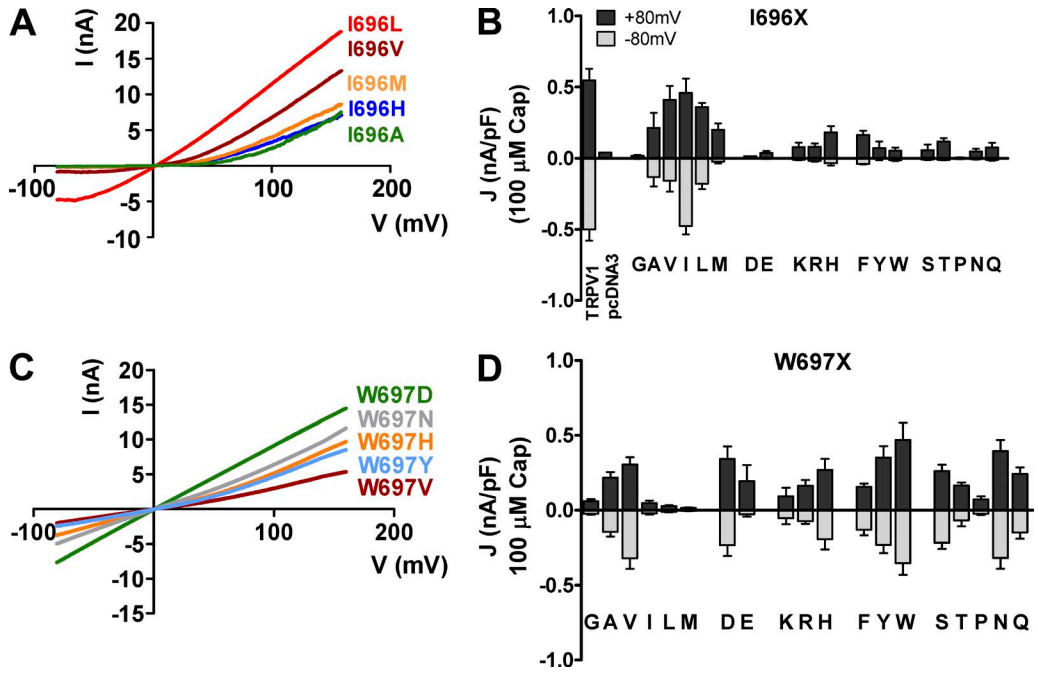


**Figure 2.** Response to capsaicin and voltage of representative I696X and W697X mutants. (A) I-V curves of ionic currents evoked by 100 µM capsaicin from representative I696X mutants. (B) Current density values at +80 and −80 mV of I696X mutants in the presence of 100 µM capsaicin. (C) I-V curves of ionic currents activated by capsaicin at 100 µM from representative W697X mutants. (D) Current density values at +80 and −80 mV of W697X mutants in the presence of 100 µM capsaicin. I-V curves were obtained using a voltage ramp protocol from −80 mV to +160 mV in 350 ms. The current density of TRPV1 wild type, I696I (I), and W697W (W) species was obtained in the presence of 1 µM capsaicin. Data are given as mean ± SEM (error bars), with *n* (number of cells) ≥ 5.

It is interesting to note that I696A and I696M mutants also exhibit an apparent decrease in the amount of the higher molecular weight characteristic of TRPV1 wild-type channels (Fig. 3 A). This band has been attributed to an *N*-glycosylated form of the protein (Wirkner et al., 2005; Winter et al., 2013). A reduction

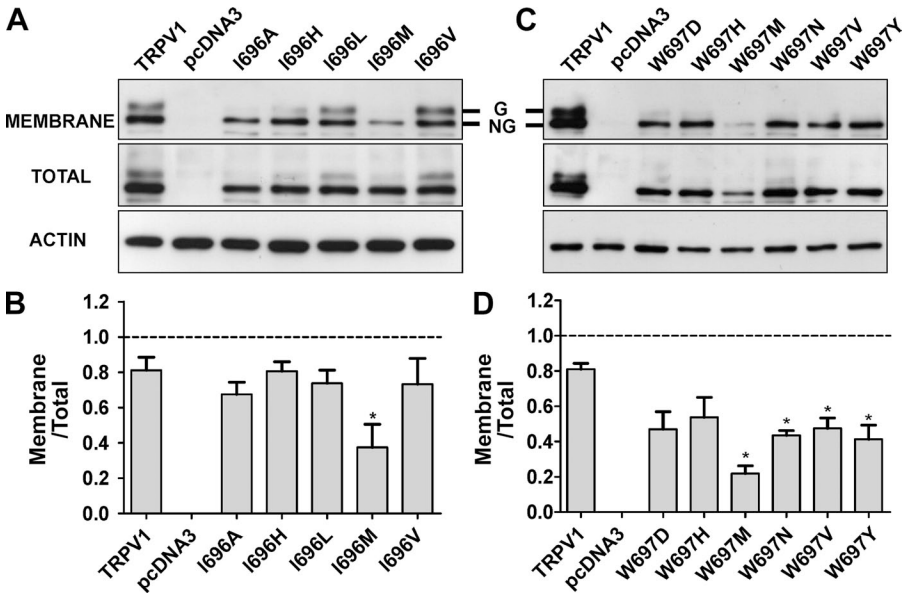


**Figure 3.** Mutation of I696X and W697X does not abrogate receptor surface expression. (A and B) Total and surface expression of representative I696X (A) and W697X (B) mutants. TRPV1 species were transiently expressed in HEK293 cells. At 48 h, cells were harvested, membrane proteins were biotinylated and purified by agarose-Streptavidin, and protein expression was analyzed by Western immunoblotting using a polyclonal anti-TRPV1 antibody. Whole cell and avidin-purified extracts were separated in 10% SDS-PAGE gels, electrotransferred to a PVDF membrane, and probed with the anti-TRPV1 antibody. Immunoblots were visualized with the ECL system. C and D denote the quantification expressed as the surface/total protein ratio of bands shown in A and B. Actin was used as a loading control. Mutants were chosen to represent the amino acid families. Data represent mean ± SEM (error bars), with *n* (number of independent experiments) = 3. *, $P < 0.05$ as compared with wild type, using a Student's *t* test.

of the *N*-glycosylated band was also observed in other nonfunctional I696X mutants (unpublished data).

For W697X mutants, we selected a representative set of mutants to evaluate if incorporation of residues with different physico-chemical properties had an impact on the total and surface protein expression. As depicted in Fig. 3 C, all mutant channels were expressed with comparable levels of total protein, except for the W697M mutant, which displayed significantly lower expression. All these W697 mutants were expressed at the cell surface, although the fraction that reached the plasma membrane was lower than that of the wild-type protein, which is consistent with the smaller ionic currents recorded for these mutant channels (Fig. 2, B and D). Note that we could not observe the double protein band characteristic of wild-type channels in the W697X mutants assayed (Fig. 3 B), even though the amount of channel that reached the membrane was significant, implying a notable reduction of *N*-type glycosylation in these mutants. This finding suggests that mutation of W697 in the TRP box might produce a conformational change in the protein subunit that somehow affected its *N*-glycosylation in the ER, although this is not sufficient to abolish surface expression and channel activity. Indeed, nonglycosylated TRPV1 channels are functional but exhibit lower responses than wild type to the activating stimuli (Wirkner et al., 2005; Cohen, 2006; Winter et al., 2013).

### Replacement of I696 by hydrophobic amino acids marginally affects voltage-dependent gating

To learn more about the functional effects of mutating the I696 site in the TRP box, we obtained the conductance-to-voltage (g-V) relationships of voltage-dependent gating for I696X functional mutants. Because voltage is a partial activator of TRPV1 channels (Matta and Ahern, 2007), we normalized the g-V curves using the maximal channel conductance ($g_{max}$), which was obtained from g-V curves in the presence of 100 µM capsaicin (Table 1). As depicted in Fig. 4 A, voltage partially activated TRPV1 channels ($P_{max} = 0.67 \pm 0.02$), with a $V_{0.5}$ of 114 ± 4 mV and a $z_g$ of 0.58 ± 0.08, in accordance with other groups (Matta and Ahern, 2007). I696X mutants slightly affected the g-V relationship, with higher $V_{0.5}$ potentials compared with wild-type channels (Fig. 4 B); this was more evident for I696M channels. As shown previously, I696A mutants barely responded to voltage (Valente et al., 2008). The gating valence, obtained from the slope of the normalized g-V curve, was not significantly altered by the amino acid changes at the I696 position (0.57–0.62 $e_o$; Fig. 4 C). These data could be used to estimate the activation energy of voltage-dependent gating at 0 mV, assuming a simple two-state model where the channel transits from a closed to an open state upon depolarization. As depicted in Fig. 4 D, only the I696M mutant significantly raised the free energy of voltage activation by 0.8 kcal/mol compared with wild-type channels. Therefore, incorporation of an aliphatic hydrophobic amino acid at I696 seems to modulate voltage-dependent gating as a function of the residue size, as indicated by the lower voltage sensitivity of I696M and I696A mutants.

### I696X mutants display voltage-dependent capsaicin responses

To further characterize the phenotype of the mutants, we also examined the g-V curves in the presence of

TABLE 1

*Voltage dependent gating and free energies of channel gating for I696X and W697X in the presence of 1 µM capsaicin*

| Channel | $V_{0.5}$[a] | $z_g$[a] | $g_{max}$[a] | $P_{min}$[b] | $\Delta G_o(I)$[c] | $\Delta G_o(V)$[d] | $\Delta G_o$[e] |
|---|---|---|---|---|---|---|---|
| | *mV* | | *nS* | | *kcal/mol* | *kcal/mol* | *kcal/mol* |
| TRPV1 | −22 ± 5 | 0.62 ± 0.08 | 124 ± 7 | 0.32 ± 0.01 | 0.20 ± 0.08 | −0.29 ± 0.06 | 0.23 ± 0.12 |
| I696A | 100 ± 10 | 0.68 ± 0.09 | 60 ± 7 | 0.003 ± 0.06 | 3.26 ± 0.38 | 1.56 ± 0.19 | 4.83 ± 0.79 |
| I696V | 81 ± 6 | 0.62 ± 0.07 | 77 ± 15 | 0.08 ± 0.05 | 1.43 ± 0.13 | 1.16 ± 0.10 | 2.59 ± 0.29 |
| I696L | 78 ± 8 | 0.64 ± 0.09 | 86 ± 10 | 0.08 ± 0.07 | 1.42 ± 0.07 | 1.16 ± 0.18 | 2.28 ± 0.38 |
| I696M | 87 ± 7 | 0.74 ± 0.07 | 79 ± 9 | 0.01 ± 0.11 | 2.69 ± 0.29 | 1.48 ± 0.15 | 4.20 ± 0.48 |
| I696H | 65 ± 9 | 0.65 ± 0.06 | 70 ± 8 | 0.08 ± 0.04 | 1.43 ± 0.18 | 0.97 ± 0.13 | 2.40 ± 0.39 |
| W697Y | 68 ± 7 | 0.90 ± 0.2 | 67 ± 16 | 0.40 ± 0.04 | 0.21 ± 0.05 | 1.34 ± 0.08 | 1.55 ± 0.11 |
| W697H | 69 ± 9 | 0.87 ± 0.3 | 62 ± 12 | 0.25 ± 0.03 | 0.64 ± 0.04 | 1.36 ± 0.11 | 2.00 ± 0.18 |
| W697V | 68 ± 6 | 0.88 ± 0.3 | 30 ± 6 | 0.23 ± 0.05 | 0.70 ± 0.05 | 1.33 ± 0.12 | 2.03 ± 0.20 |
| W697D | 68 ± 4 | 0.71 ± 0.1 | 133 ± 11 | 0.09 ± 0.02 | 1.34 ± 0.10 | 1.25 ± 0.14 | 2.59 ± 0.44 |
| W697N | 73 ± 8 | 0.75 ± 0.2 | 106 ± 13 | 0.03 ± 0.01 | 2.06 ± 0.07 | 1.26 ± 0.13 | 3.32 ± 0.34 |

[a]The parameter values obtained from the best fit of the g-V curves to a Boltzmann distribution (Figs. 5 B and 6 A). Free energies were estimated assuming a two-state gating model.

[b]$P_{min}$ denotes the normalized conductance at hyperpolarized potentials ($g_{min}/g_{max}$), where $g_{min}$ has been obtained for the best fit of the g-V curve to a Boltzmann distribution.

[c]The free energy of the voltage-independent component, obtained as $-RT \ln[(P_{min}/(1 - P_{min})]$.

[d]The free energy of the voltage-dependent component, obtained as $z_g F V_{0.5}$.

[e]The total free energy of the gating process, obtained as $\Delta G_o(I) + \Delta G_o(V)$.

Data are given as mean ± SEM, with $n \geq 5$.

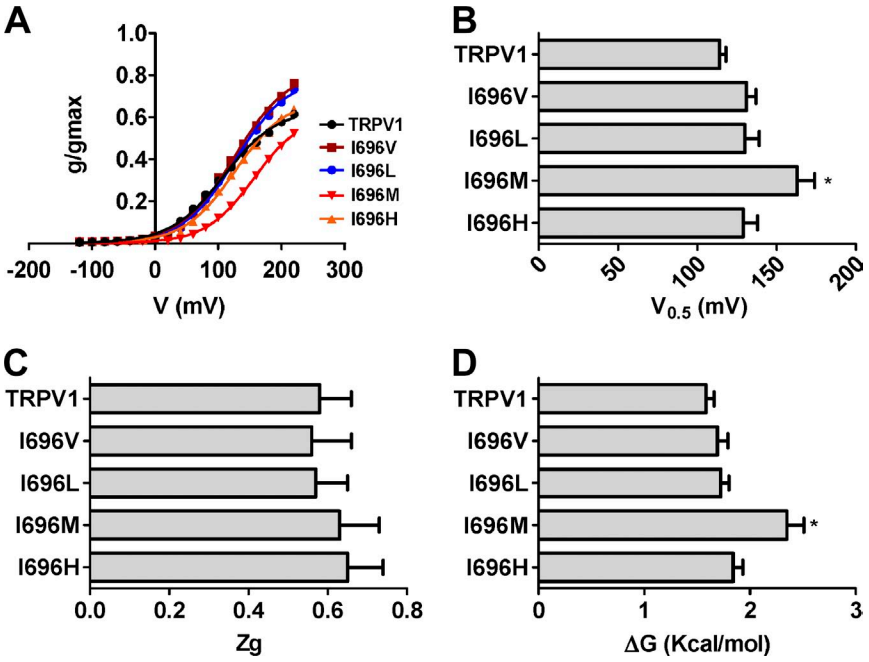


**Figure 4.** Mutation of I696 to hydrophobic amino acids affects voltage sensing and the energetics of channel gating. (A) Normalized g-V relationships for I696X voltage-responsive mutants. Solid lines depict the best fit to a Boltzmann distribution to obtain the $V_{0.5}$ and $z_g$ values. (B) $V_{0.5}$ values of the different I696X mutants obtained from the g-V curves. (C) $z_g$ values of the different I696X mutants obtained from the g-V curves. (D) $\Delta G_o$ values at 0 mV for the I696X obtained considering a simple two-state model between a closed and an open state. g-V curves were normalized with respect to the true $g_{max}$ of the channel obtained in the presence of 100 µM capsaicin (Table 1). Data are given as mean ± SEM (error bars), with *n* (number of cells) ≥ 5. *, $P < 0.05$ as compared with wild type, using the nonparametric Wilcoxon test.

1 and 100 µM capsaicin (Fig. 5, A and B) to evaluate the responses to nonsaturating and saturating vanilloid concentrations. Both g-V curves were normalized using the maximal channel conductance obtained in the presence of 100 µM capsaicin. TRPV1 channels exposed to 1 µM capsaicin displayed significant voltage-independent gating at negative membrane potentials ($P_{min}$ = 0.32 ± 0.08; Table 1), along with voltage dependency at depolarizing voltages (Fig. 5 A), which is in agreement with other groups (Matta and Ahern, 2007). In contrast, I696X mutants displayed mostly voltage-dependent responses, with modest voltage-independent gating at negative potentials ($P_{min}$ < 10%). Analysis of the $V_{0.5}$ revealed similar values for all mutants, showing the higher $V_{0.5}$ of the I696A mutant (Fig. 5 C). The presence of the vanilloid, however, did not alter the gating valence of the voltage-dependent component ($z_g \approx 0.6–0.7\ e_o$; Table 1). These results yielded a free energy change, assuming a two-state model (Fig. 5 D), with a profile that closely resembled that of $V_{0.5}$.

An incremental increase of the capsaicin concentration to saturation (100 µM) fully activated TRPV1 channels

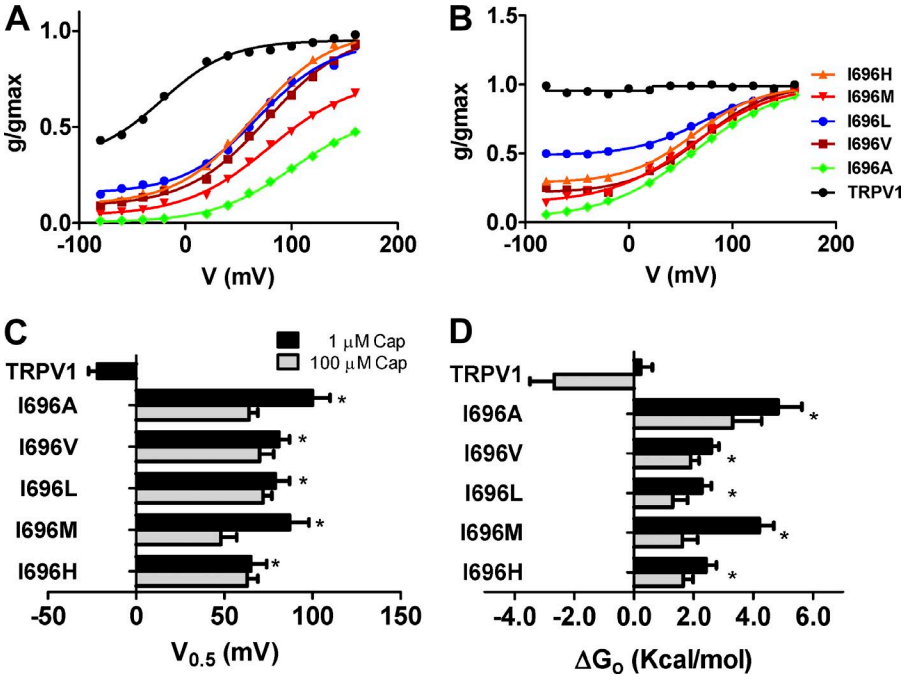


**Figure 5.** I696X mutants display an altered response to capsaicin and voltage. (A and B) Normalized g-V curves obtained in the presence of 1 µM (A) and 100 µM (B) capsaicin. Solid smooth lines depict the best fit to a Boltzmann distribution to obtain the $V_{0.5}$ and $z_g$ values. (C) $V_{0.5}$ values of the different I696X mutants obtained from the G-V curves at the vanilloid concentrations used. (D) $\Delta G_o$ values obtained as the sum of the voltage-dependent components at 0 mV ($\Delta G_o(V)$) and independent ($\Delta G_o(I)$) components considering a simple two-state model between a closed and open state (Tables 1 and 2). g-V curves were normalized with respect to the true $g_{max}$ of the channel obtained in the presence of 100 µM capsaicin (Table 2). Data are given as mean ± SEM (error bars), with *n* (number of cells) ≥ 5. *, $P < 0.05$ as compared with wild type using the nonparametric Wilcoxon test.

in a voltage-independent manner, and moved the g-V curves of I696X mutants slightly leftward, which resulted in activation of these species at marginally lower voltages (Fig. 5, B and C; Table 2). Notably, at this vanilloid concentration, I696V and I696H, and, more prominently, I696L, displayed significant voltage-independent gating at hyperpolarized potentials (Table 2). Inspection of the $P_{min}$ and free energy values further imply a partial correlation between the size/volume of the amino acid incorporated in I696 and the channel response to saturating vanilloid concentration that can be ranked, from best to worst, as Ile > Leu > Val = His > Met > Ala (Fig. 5, B and D).

### W697X mutants exhibit voltage-dependent capsaicin activation

To learn more on the role of position W697 in channel gating, we also obtained the normalized g-V curves of representative W697X mutants in the presence of 1 and 100 µM of capsaicin. Fig. 6 shows that all mutants tested displayed voltage-dependent capsaicin responses at 1.0 µM (Fig. 6 A). Notably, differences between mutants are evident at the $P_{min}$ and $P_{max}$ values. W697Y displays the largest voltage-independent activation by capsaicin ($P_{min}$ = 0.40) and the highest $P_{max}$ (1.0). Conversely, mutants W697D and W697N exhibited the lowest $P_{min}$ and $P_{max}$ values (Fig. 6 A). These two mutants displayed higher $g_{max}$ values than the other (Table 1). Fitting the normalized g-V curves to a Boltzmann distribution revealed midpoint voltages ($V_{0.5}$) of 68–75 mV (Fig. 6 B) and $z_g$ of 0.7–0.9 $e_o$ for all mutants tested (Table 1), with no significant differences among the different mutant species. These values resulted in free energies of activation for mutants that varied from 1.5–3.0 kcal/mol (Fig. 6 C and Table 1).

At 100 µM capsaicin, all W6967X mutants exhibit an increase in $P_{min}$ >0.5, which is more evident for W697D and W697N (Fig. 6 B and Table 2). These mutants displayed normalized g-V curves that were largely voltage independent ($P_{min}$ > 0.7; Fig. 6 B), resembling that of wild-type channels. Normalized g-V curves are well described by the Boltzmann distribution, giving $V_{0.5}$ values for all mutants between 50 and 70 mV, and $z_g$ of 0.7–0.9 $e_o$ (Fig. 6 C and Table 2). The W697D mutant displayed the lowest $V_{0.5}$, which resulted in a negative free energy of activation, akin to wild-type channels (Fig. 6 D and Table 1). It should be noted, however, that estimates of voltage-dependent parameters for W697D and W697N at 100 µM may be inaccurate because of the large voltage-independent gating displayed by these mutants in the range of voltages explored.

### Mutation of positions I696 and W697 significantly affects allosteric coupling

Although we have previously used a simple two-state model to determine the impact of the mutations on channel gating, this probably reflects a simplification, as TRPV1 gating is a complex allosteric mechanism involving a large number of states. Allosteric models have been proposed to account for the voltage, temperature, and capsaicin gating of thermo-TRP channels (Brauchi et al., 2004; Matta and Ahern, 2007; Latorre et al., 2007; Yao et al., 2010a; Voets, 2012) using a similar conceptual basis and formalism to that used for large conductance potassium channels (Horrigan and Aldrich, 2002; Wu et al., 2009). Basically, allosteric activation mechanisms for polymodal receptors

TABLE 2

*Voltage dependent gating and free energies of channel gating for I696X and W697X in the presence of 100 µM capsaicin*

| Channel | $V_{0.5}$[a] | $z_g$[a] | $g_{max}$[a] | $P_{min}$[b] | $\Delta G_o(I)$[c] | $\Delta G_o(V)$[d] | $\Delta G_o$[e] |
|---|---|---|---|---|---|---|---|
| | *mV* | | *nS* | | *kcal/mol* | *kcal/mol* | *kcal/mol* |
| TRPV1 | NA | NA | 124 ± 7 | 0.95 ± 0.01 | −2.67 ± 0.81 | NA | −2.67 ± 0.81 |
| I696A | 64 ± 5 | 0.55 ± 0.06 | 60 ± 7 | 0.01 ± 0.06 | 2.67 ± 0.63 | 0.63 ± 0.15 | 3.30 ± 0.98 |
| I696V | 70 ± 8 | 0.75 ± 0.05 | 77 ± 15 | 0.21 ± 0.05 | 0.77 ± 0.12 | 1.33 ± 0.11 | 1.90 ± 0.31 |
| I696L | 72 ± 7 | 0.76 ± 0.09 | 86 ± 10 | 0.50 ± 0.07 | 0.05 ± 0.02 | 1.26 ± 0.25 | 1.30 ± 0.51 |
| I696M | 48 ± 9 | 0.79 ± 0.04 | 79 ± 9 | 0.15 ± 0.11 | 1.05 ± 0.05 | 0.57 ± 0.12 | 1.62 ± 0.51 |
| I696H | 63 ± 6 | 0.79 ± 0.07 | 70 ± 8 | 0.29 ± 0.04 | 0.52 ± 0.09 | 1.13 ± 0.20 | 1.65 ± 0.36 |
| W697Y | 49 ± 9 | 0.85 ± 0.3 | 67 ± 16 | 0.51 ± 0.05 | −0.02 ± 0.01 | 0.98 ± 0.09 | 0.95 ± 0.17 |
| W697H | 66 ± 8 | 0.87 ± 0.4 | 62 ± 12 | 0.67 ± 0.03 | −0.40 ± 0.06 | 1.30 ± 0.12 | 0.90 ± 0.14 |
| W697V | 68 ± 7 | 0.89 ± 0.3 | 30 ± 6 | 0.57 ± 0.04 | −0.24 ± 0.03 | 1.30 ± 0.18 | 1.06 ± 0.19 |
| W697D | 8 ± 11 | 0.72 ± 0.2 | 133 ± 11 | 0.87 ± 0.02 | −1.05 ± 0.08 | 0.14 ± 0.06 | −0.91 ± 0.61 |
| W697N | 57 ± 10 | 0.81 ± 0.3 | 106 ± 13 | 0.81 ± 0.03 | −0.80 ± 0.07 | 1.11 ± 0.36 | 0.31 ± 0.31 |

[a]The parameter values obtained from the best fit of the g-V curves to a Boltzmann distribution (Figs. 5 B and 6 A). Free energies were estimated assuming a two-state gating model.

[b]$P_{min}$ denotes the normalized conductance at hyperpolarized potentials ($g_{min}/g_{max}$), where $g_{min}$ has been obtained for the best fit of the g-V curve to a Boltzmann distribution.

[c]The free energy of the voltage-independent component, obtained as $-RT \ln[(P_{min}/(1 - P_{min})]$.

[d]The free energy of the voltage-dependent component, obtained as $z_g F V_{0.5}$.

[e]The total free energy of the gating process, obtained as $\Delta G_o(I)+\Delta G_o(V)$.

Data are given as mean ± SEM, with $n \geq 5$. NA, not applicable.

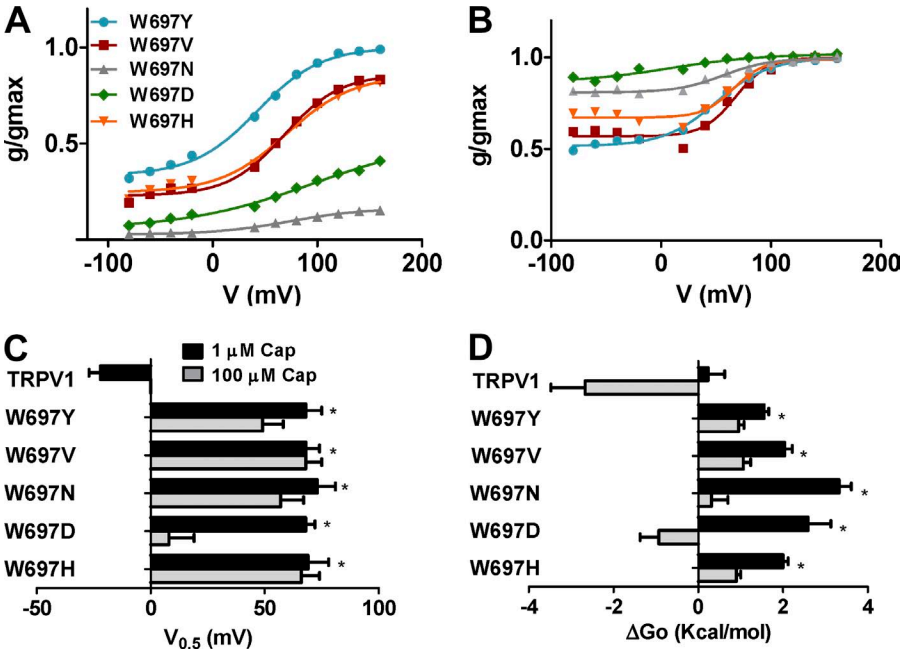


**Figure 6.** Mutation of W697 alters the response to capsaicin and voltage. (A and B) Normalized g-V relationships for selected W697X mutants in the presence of 1 µM (A) and 100 µM (B) capsaicin. Solid smooth lines depict the best fit to a Boltzmann distribution to obtain the $V_{0.5}$ and $z_g$ values. (C) $V_{0.5}$ values of the different W697X mutants obtained from the g-V curves. (D) $\Delta G_o$ values obtained as the sum of the voltage dependent components at 0 mV ($\Delta G_o(V)$) and independent ($\Delta G_o(I)$) components considering a simple two-state model between a closed and open state. g-V curves were normalized with respect to the true $g_{max}$ of the channel obtained in the presence of 100 µM capsaicin (Tables 1 and 2). Data are given as mean ± SEM (error bars), with $n$ (number of cells) ≥ 5. *, $P < 0.05$ as compared with wild type, using the nonparametric Wilcoxon test.

have assumed the existence of independent sensors that are coupled to gate the channel (Fig. 7). For simplicity we use the same nomenclature as Matta and Ahern (2007). Because we have evaluated the activity of all mutants at room temperature (22 ± 1°C), we assume that the temperature sensor has remained in the resting state and has not contributed significantly to channel gating. Thus, we only considered an active role in channel gating of the voltage and capsaicin sensors (Fig. 7 A). In addition, we assume that these sensors move simultaneously, giving rise to an eight-state allosteric model (Fig. 7 A). According to this model, the equilibrium constant J governs the transitions between the resting ($R_V$) and active ($A_V$) states of the voltage sensor, whereas the constant Q determines the equilibrium between the unbound (U) and bound (B) states of the capsaicin binding site, and L drives the transitions between the closed (C) and open (O) states (Fig. 7 A). Voltage sensors and capsaicin binding sites are coupled to pore opening by the allosteric constants D and P, respectively; and to each other by E.

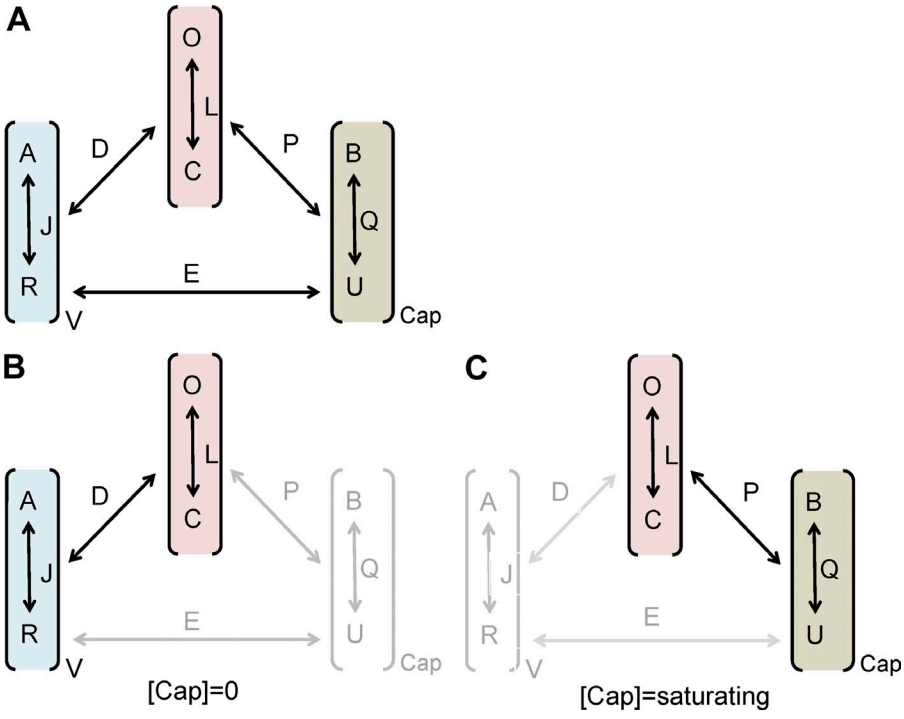


**Figure 7.** Allosteric model of activation of TRPV1 channels by voltage and capsaicin. (A) The model considers the action of the voltage sensor that can be in a resting ($R_V$) or activated state ($A_V$), and the ligand sensor that can be in the unbound (U) or bound state. The voltage sensor has an equilibrium constant J, the ligand sensor is characterized by the equilibrium constant Q, and the ionic pore by the equilibrium constant L. In addition, the model assumes that the voltage sensor is coupled to the pore by the allosteric constant D, the ligand sensor is coupled to the pore by the allosteric constant P, and that both sensors are coupled by the allosteric constant E. Because we performed all our studies at room temperature (22°C), we assumed that the temperature sensor would have a negligible contribution, remaining in its resting state. (B) In the absence of agonist, channel gating is driven by the activation of the voltage sensor; at saturating concentration of capsaicin (C), channel gating is largely voltage independent.

In the absence of capsaicin, channel gating is driven by the activation of the voltage sensors (Fig. 7 B). Assuming that all voltage sensors activate simultaneously, the open probability for voltage gating is given by Horrigan and Aldrich (2002), Brauchi et al. (2004), and Matta and Ahern (2007):

$$P_o(V) = \frac{1}{1 + \frac{(1+J)}{L(1+JD)}} \text{ where } J = J_o e^{\frac{z_g FV}{RT}}. \quad (1)$$

$J_o$ denotes the equilibrium constant at 0 mV, and $z_g$ denotes the gating valence of the activation process. We fitted our normalized g-V curves to this model and found that it appropriately described the experimental data for wild-type channels (Fig. 8). The best fit was obtained with the following values for the constants: $J_o$ = 0.021, L = $5.3 \times 10^{-4}$, D = 4,500, and $z_g$ = 0.60, which are in good agreement with those reported by Matta and Ahern (2007). For I696X mutants, the values obtained for $z_g$ and the equilibrium constants $J_o$ and L were virtually identical to those of TRPV1 wild type (Table 3). The main effect of mutating position I696 was the modulation of allosteric coupling constant D.

The free energy of channel activation can be estimated from the allosteric model by Voets (2012) and Chowdhury and Chanda (2013):

$$\Delta G_o = -RT \ ln\left(\prod_{i=1}^{n} K_i\right), \quad (2)$$

where RT = 0.58 kcal/mol at 22°C, and $K_i$ is the equilibrium constant considered in the model. For the voltage activation these would be $J_o$, D, and L. As reported in Table 3, the free energy was 1.5–2.1 kcal/mol, which is akin to that of wild-type channels. Notably, these free energies are similar to those derived from a two-state model for gating, which is consistent with the notion that the free energy of voltage–mediated gating is defined primarily by the channel gate, and can be fairly described by a two-state model.

We next evaluated the allosteric mechanisms of gating in the presence of capsaicin. For this purpose, we introduced the equilibrium between the capsaicin bound and unbound states (Fig. 7), governed by the constant Q = [capsaicin]/$K_d$, where $K_d$ denotes the capsaicin dissociation constant, which is different from the $EC_{50}$ obtained from the dose–response curves (Matta and Ahern, 2007). The open probability when voltage and capsaicin act together can be described by the relation:

$$P_o(V, Capsaicin) = \frac{1}{1 + \frac{(1+J+Q+JQE)}{L(1+JD+QP+JDQPE)}}. \quad (3)$$

A problem with TRPV1 channels is that we do not clearly know the number of capsaicin molecules needed to gate the channel. However, akin to Brauchi et al. (2004) and Matta and Ahern (2007), we assume that all binding sites need to be occupied for activation. However, at variance with these studies, we also considered the existence of an allosteric coupling between the voltage and capsaicin sensors characterized by a coupling constant E. If both sensors operated independently, then E = 1. A reason for considering the existence of this

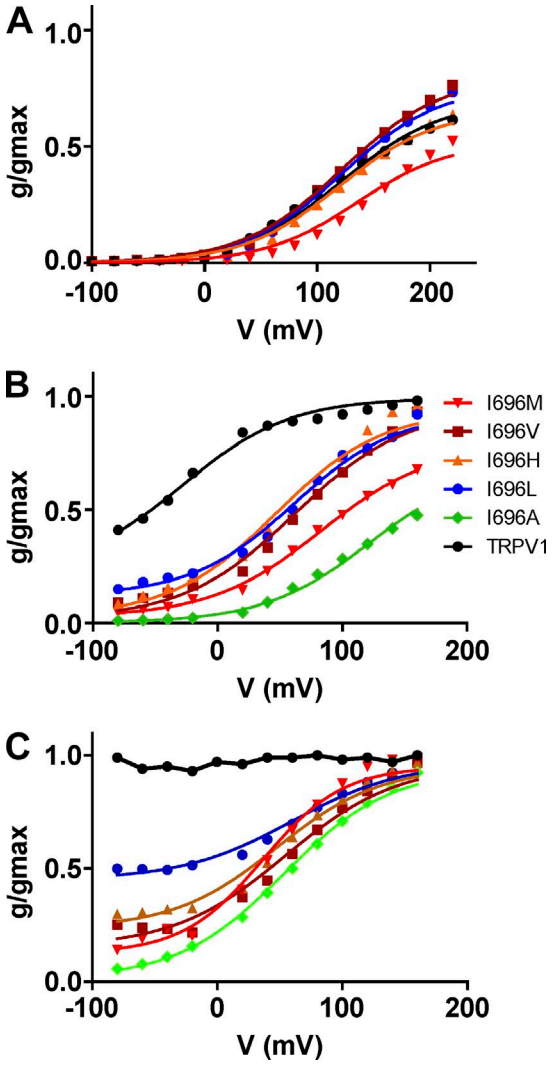


**Figure 8.** The proposed allosteric model reproduces the experimental data of TRPV1 wild type and I696X mutants. The figure depicts the normalized g-V curves obtained for the I696X mutants in the absence (A) and presence of capsaicin at 1 µM (B) and 100 µM (C). Solid lines depict the best fit to the allosteric model. Normalized g-V curves in the absence of capsaicin were fitted to Eq. 1, and results are given in Table 3. Normalized g-V curves in the presence of capsaicin were fitted to Eq. 3, fixing the values for the equilibrium constants obtained in the absence of capsaicin: $J_o$ = 0.021, L = $5.0 \times 10^{-4}$, $K_d$ = $10^{-5}$, and $z_g$ = 0.6. The value of E given by the analysis was virtually 1 and, therefore, was kept constant to this value. The values obtained for allosteric constants P and D and free energy are depicted in Table 4.

TABLE 3

*Allosteric model parameters for I696X in the absence of capsaicin*

| Channel | $J_0$ | $z_g$ | L | D | $\Delta G_o$ |
|---|---|---|---|---|---|
| | | | | | *kcal/mol* |
| TRPV1 | 0.021 | 0.60 | 0.00053 | 4,500 | 1.7 |
| I696V | 0.018 | 0.60 | 0.00047 | 8,500 | 1.5 |
| I696L | 0.019 | 0.60 | 0.00050 | 6,000 | 1.6 |
| I696M | 0.018 | 0.62 | 0.00049 | 2,000 | 2.1 |
| I696H | 0.021 | 0.60 | 0.00049 | 4,000 | 1.8 |

Normalized g-V curves (Fig. 8 A) were fitted to the Eq. 1, and free energies were obtained using Eq. 2.

coupling is that in TRPV1 channels both sensors appear to overlap in the same protein regions, which makes more than a plausible a crosstalk between them. Furthermore, Jara-Oseguera and Islas (2013) recently showed that voltage and temperature sensors in thermo-TRP channels are coupled.

Using Eq. 3, we first fitted the normalized g-V curves of I696X mutants obtained in the presence of 100 µM (Fig. 8). Because the model is based on independent modules, we fixed the values of $J_o$, $z_g$, and L obtained in the absence of ligand. In addition, we used the value of $K_d$ reported by Matta and Ahern (2007), namely $10^{-5}$ µM. Under these conditions, the model is reduced to three parameters: D, P, and E. Our experimental data for I696X mutants were well described by E = 1, which indicates that the voltage and ligand sensor are not coupled. The value of P was higher for I696L (P = 1,800) and lower for I696A (P = 32; Table 4), in agreement with their differential response of the mutants to the vanilloid. Under these conditions, fitting the experimental g-V curves to the model required a decrease in the value of the allosteric constant D. Hence, the I696L exhibited the lowest value (D = 38) while the I696A displayed the highest (D = 1,300). A decrease in the amount of capsaicin to 1 µM resulted in an increment of the allosteric coupling constant D for all mutants, except for I696A, which indicates a major contribution of voltage to gating (Fig. 8 and Table 4). The values of the allosteric coupling constant P and E were unchanged upon reduction of the capsaicin concentration. Collectively, these results indicate that mutation of I696 to hydrophobic residues mostly alters the allosteric coupling constants for voltage and ligand. Overall, these data further support the finding that mutation of amino acid I696 in the TRP domain has a significant impact on the allosteric mechanisms of activation by affecting the coupling of pore opening to the activating sensors. Furthermore, the energetic profile substantiates the notion that position I696 in the TRP box is optimized to have an Ile residue for optimal channel activation.

A similar analysis was performed for the selected set of W697X functional mutants (Fig. 9). We assumed that constants $J_o$, L, and $K_d$ were not altered by the mutations, and used those obtained for TRPV1 wild-type channels. First, we analyzed the normalized g-V curves

TABLE 4

*Allosteric model parameters for I696X and W697X mutants in the presence of 1 and 100 µM capsaicin*

| Channel | 1 µM | | | 100 µM | | |
|---|---|---|---|---|---|---|
| | D | P | $\Delta G_o$ | D | P | $\Delta G_o$ |
| | | | *kcal/mol* | | | *kcal/mol* |
| TRPV1 | 370 | 3,000 | −1.45 | NA | NA | NA |
| I696A | 1,400 | 32 | 0.40 | 1,300 | 32 | 0.45 |
| I696V | 1,008 | 460 | −0.78 | 144 | 460 | 0.33 |
| I696L | 131 | 1,800 | −0.46 | 38 | 1,800 | 0.25 |
| I696M | 373 | 480 | −0.21 | 134 | 480 | 0.38 |
| I696H | 504 | 720 | −0.76 | 61 | 720 | 0.46 |
| W697Y | 30 | 2,200 | 0.17 | 50 | 9,500 | −0.96 |
| W697H | 30 | 4,000 | −0.15 | 18 | 7,200 | −0.21 |
| W697V | 18 | 2,900 | 0.31 | 25 | 6,100 | −0.31 |
| W697D | 10 | 13,000 | −0.25 | 8 | 2,300 | 0.92 |
| W697N | 10 | 8,500 | 0.03 | 6 | 6,300 | 0.50 |

Normalized g-V curves in the presence of capsaicin were fitted to Eq. 3. For I696X and wild type, the values for the equilibrium constants were fixed to those obtained in the absence of capsaicin: $J_o = 0.021$, $L = 5.0 \times 10^{-4}$, $K_d = 10^{-5}$, and $z_g = 0.6$. For W697X mutants, these values were the same, except for $z_g = 0.80$, which was taken from the Boltzmann fits. The value of E given by the analysis for all mutants was virtually 1 and, therefore, was kept constant to this value. NA, not applicable.

in the presence of 100 µM capsaicin to obtain the values of the allosteric coupling constants D, P, and E (Fig. 9). As for wild-type channels and I696X mutants, the eight-state allosteric model described fairly well the experimental data of W6967X mutants using the equilibrium constants of the wild-type channel (Fig. 9). In the presence of 100 µM, the model was best described by a large contribution of ligand-evoked gating, as indicated by the large values of the coupling constant P (Table 4), and a modest participation of voltage gating as indicated by the low values of the allosteric constant D. At variance with I696X mutants analyzed, a decrease in the capsaicin concentration to 1 µM did not result in a significant increment of the allosteric constant D in W697X mutants (Fig. 9), which suggests that mutation of W697 severely uncouples the voltage sensor form pore opening (Table 4). This result is consistent with the higher voltage values that are needed to activate the W697X mutants in the absence of capsaicin.

## DISCUSSION

Extensive structure–function analysis of TRPV1 channels has been performed with the aim of identifying receptor domains involved in stimuli sensing and understanding their contribution to channel gating (Winter et al., 2013). These studies have mapped potential regions involved in voltage, capsaicin, pH, and temperature sensing, along with domains that interact with proteins and phosphoinositides. Furthermore, the TRP domain, a region implicated in subunit oligomerization, has been also reported (García-Sanz et al., 2004, 2007). Interestingly, this domain appears to exhibit a dual function, as it also participates in the functional coupling of stimuli sensing and pore opening. Mutations within the highly conserved core of the TRP domain (referred to as the TRP box), affected all modes of TRPV1 channel gating, even though this region is located far from most of the putative regions acting as channel sensors (Valente et al., 2008). These findings signaled the TRP box as a pivotal receptor domain in the allosteric mechanism of channel activation by coupling the energy of the activating stimuli to open the pore. To address this fundamental question, we mutated the most critical positions (I696 and W697; Fig. 1 A) in the TRP box to 18 L-amino acids, with the aim of furthering our understanding of the role of the TRP domain in the allosteric linkage of sensors and the channel gate. We focused on studying voltage and capsaicin activation at a constant temperature (22°C).

The salient contribution of this study is that mutation of I696 and W697 primarily affects the allosteric coupling constants of the voltage and ligand sensors to the channel pore, without altering the sensors and pore equilibrium constants. Our results show that position I696 was only tolerant to substitutions by hydrophobic amino acids, and uncover an effect of the amino acid size at I696 in channel activation. Functional I696X mutants exhibited altered channel gating, characterized by a lower response to the activating stimuli. Smaller or larger amino acids than I696 negatively impacted channel activity, resulting in lower current densities and higher free energy of activation. In marked contrast, position W697 tolerated virtually all substitutions, except large hydrophobic amino acids. Most W697X mutants displayed channel activity in the presence of saturating concentrations of capsaicin. Intriguingly, none of the W697X mutants could be activated by depolarizing voltages as high as 240 mV in the absence of the vanilloid, which suggests a complete uncoupling of voltage sensing and gate opening in these mutants. Collectively, these findings support the tenet that the TRP box in TRPV1, and probably in other TRP channels, is an important molecular determinant of channel activation that pivotally contributes to the energetics of channel gating by modulating the allosteric coupling constants of channel sensors and the pore.

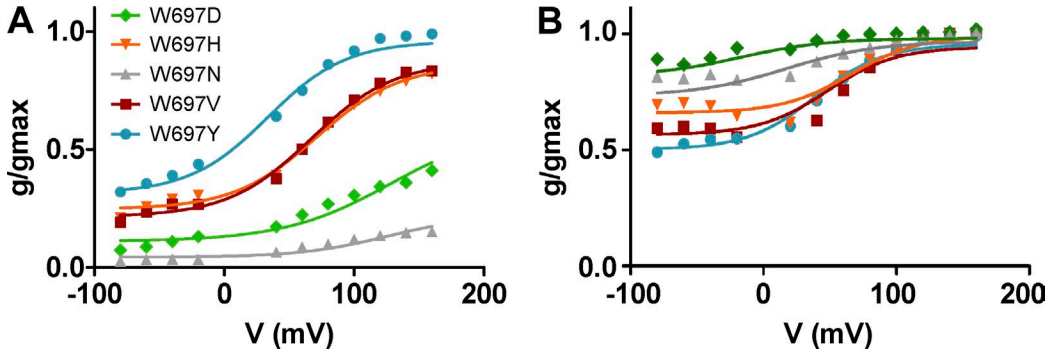


**Figure 9.** The proposed allosteric model reproduces the experimental data of W697X mutants. The figure depicts the normalized g-V curves obtained for the W697X mutants in the presence of presence at 1 µM (A) and 100 µM (B) of capsaicin. The solid lines depict the best fit to the allosteric model. Data were fitted to Eq. 3, fixing the following values for the equilibrium constants: $J_o = 0.021$, $L = 5.0 \times 10^{-4}$, $K_d = 10^{-5}$, $z_g = 0.8$, and $E = 1$. The values obtained for allosteric constants P and D and free energy are depicted in Table 4.

It is interesting to note that mutation of I696 and W697 did not significantly affect the recombinant protein expression of most channel species in HEK293 cells. Nonetheless, the W697M mutant, and likely the other W697X mutants that displayed a poor functional response to 100 µM capsaicin (Fig. 2 B), appear to display a reduced surface expression, although the channel that reached the membrane was activated by the vanilloid. It is noteworthy that all W697X mutants analyzed by Western immunoblotting did not display the characteristic *N*-glycosylated TRPV1 band in the total extract and surface-expressed fraction, which suggests that mutation of this position may have induced a conformational change in the receptor subunit that affected the *N*-glycosylation of the channel in the endoplasmic reticulum. Most likely, the lack of the *N*-glycosylated form in W697 mutants reduced the surface expression of these channels, which is consistent with their lower capsaicin efficacy and smaller current densities as compared with wild-type channels. This finding implies that mutation of W697 in the TRP domain of TRPV1 might modulate protein folding in the S4–S6 region, perhaps by perturbing interactions with the S4–S5 linker that contribute to defining the quaternary structure of the channel in this region, or by altering the tetrameric assembly of channel subunits, considering the role of the TRP segment as an association domain (García-Sanz et al., 2004). However, these conformational changes, if present, should be subtle because our functional data are well described by equilibrium constants for the voltage sensor and pore that are virtually identical to TRPV1 wild type. Clearly, additional data are needed to fully understand the mechanism involved in the modulation of *N*-glycosylation of the protein by mutation of W697, and a potential role of the TRP domain in protein conformation. Nevertheless, this modulation of the protein conformation may underlie the effects observed in the allosteric coupling required for channel activation.

A question that emerges is: how is it that the TRP box may modulate functional coupling in TRPV1? In the absence of a three dimensional structure for the channel, it is rather unfeasible to provide a compelling mechanism. One can envision and hypothesize several possibilities that could account for the impact of mutating the TRP box in channel gating. In the four-strand, parallel coiled-coil model proposed for the TRP domain (García-Sanz et al., 2004, 2007; Fernández-Ballester and Ferrer-Montiel, 2008), amino acids I696 and W697 are located at the a and b positions (Fig. 1 A), where they can mediate intersubunit interactions important for the allosteric coupling of the activating stimuli to the opening of the channel gate. Our observation that I696 could only be replaced by hydrophobic amino acids, and the effect of the amino acid volume in channel gating evoked by voltage and capsaicin, are consistent with location I696 in the hydrophobic core of a coiled-coil fold. Incorporation of smaller and larger amino acids than Ile may strengthen the hydrophobic interactions at this level of the coiled coil, raising the energy of channel gating. The impact in the allosteric coupling constants (D and P) exhibited by functional I696X mutants is consistent with this interpretation, which gives support to the proposed helical organization of the TRP domain.

The location of W697 at the b position of the coiled-coil arrangement also appears to be compatible with the impact of its mutation on channel function. This amino acid could be located at the helical interface involved in intersubunit interactions. Alternatively, it could be more externally oriented for interacting with other subunit domains such as the S4–S5 linker or the S2–S3 loop, or even a region in the N-terminal domain. Our finding that W697 could be replaced by virtually all amino acids without losing channel function argues against a critical contribution to coiled-coil intersubunit interactions, and instead implies a more external spatial localization that would be more tolerant to substitutions. It is noteworthy that, although virtually all W697X mutants responded to a variable extent to capsaicin, all of them required unreachable voltages for channel activation in the absence of capsaicin. However, capsaicin responses displayed weak voltage dependency that, intriguingly, was marginally affected by the vanilloid concentration. A putative interaction of W697 with the S4–S5 linker during gating could explain the effect of the mutants. In this regard, the S4–S5 linker displays the presence of three positively charged residues (K571, R575, and R579) that could create a positive surface potential for a π-cation–like interaction with W697. In support of this notion, substitution of W697 by negatively charged and polar residues was better tolerated than by positively charged and large hydrophobic amino acids. This interaction, optimal for a Trp residue because of its polarity and volume, could be essential for coupling the movement of the voltage sensor to the opening of the pore. A similar mechanism was proposed for Kv channels, where gating required a compatible S4–S5 linker and the region adjacent to the channel gate (Labro et al., 2008, 2011). However, the distance of the TRP box (>10 Å) from the pore gate in the proposed parallel coiled-coil model for the C terminus of TRPV1 is incompatible with this mechanism because it would require a large conformational change in the TRP domain to approach W697 to the S4–S5 linker (Fernández-Ballester and Ferrer-Montiel, 2008). However, should the TRP domain be structured as an antiparallel coiled coil, this would position amino acid W697 near the S4–S5 linker, which is consistent with the role of this residue in voltage gating. In addition, the proposed interaction of amino acids near this region with $PIP_2$ in the inner leaflet of the membrane could further approximate this domain to the channel gate, facilitating its interaction with protein domains located in the membrane interface, such

as parts of the S4–S5 linker (Brauchi et al., 2007; Labro et al., 2008; Ufret-Vincenty et al., 2011). Thus, the current model of the C terminus probably requires revision in light of the role played by residues in the TRP domain on coupling the activating stimuli to the opening of the channel pore. Evidently, structural data are necessary to unequivocally unveil the structural layout and interactions of the W697 and I696 residues, which is essential to unambiguously disclose the role of the TRP domain in channel function.

While this paper was under review, Liao et al. (2013) and Cao et al. (2013) reported on the structure of the TRPV1 channel at 3.4-Å resolution, using cryo-microscopy in the absence and presence of agonists, respectively. This structure shows that the TRP domain adopts an α-helix configuration that runs parallel to the inner leaflet of the plasma membrane, interacting with the S4–S5 linker, the pre-S1 helix segment, and probably with the S2–S3 linker as well (missing in the published structure). The layout and interactions of residues I696 and W697 in the channel structure is consistent with our results on the impact of their mutation on channel function. Interestingly, the invariant W697 in the TRP box forms a hydrogen bond with the main-chain carbonyl oxygen of F559 in the beginning of the S4–S5 linker (Cao et al., 2013; Liao et al., 2013), which is in agreement with the severe effect on voltage sensing when mutating this residue to any other amino acid. Therefore, our findings, along with the reported TRPV1 structure, strengthen the tenet of a critical role of the first half of the TRP domain in the allosteric coupling of stimuli sensing and gate opening.

In conclusion, our findings strongly substantiate the tenet that the TRP domain in TRPV1 is a pivotal structural determinant of allosteric channel gating. Here we provided evidence that mutations in two important sites of this region, located in the so-called TRP box, primarily modulate the allosteric constants that couple stimuli sensing and gate activation. Notably, a critical contribution of W697 in coupling voltage-dependent gating was uncovered. Note that a Tryptophan residue is absolutely conserved in this position of the TRP box in all the TRP channels (TRPC, TRPM, and TRPV) bearing a TRP domain, which further supports a central role in channel function. It is interesting to note that the mutation W692G in the TRP box of TRPV3, which alters the response of the channel to 2-ABP, has been linked as a cause of the Olmsted syndrome, a rare congenital disorder characterized by diverse skin alterations and alopecia (Lin et al., 2012), further substantiating the relevant role of the TRP box in TRP channel function. Although structural information is required for a full understanding of the molecular details involved in channel gating, our results help to define the role of the TRP domain in polymodal activation. Furthermore, our results lend support to data showing that interference with the interactions at the level of the TRP domain during gating represents a novel strategy to modulate channel gating in this family of ion channels.

We thank Prof. D. Julius for kindly providing the rat TRPV1 cDNA.

This work has been supported by grants from the Spanish Ministerio de Economía y Competitividad (MINECO: BFU2009-08346 and BFU2012-39092-C02-01 to A. Ferrer-Montiel, and BFU2011-25920 to J.M. González-Ros; and the CONSOLIDER-INGENIO 2010 Program: CSD2008-00005 to A. Ferrer-Montiel and J.M. González-Ros), and the Generalitat Valenciana PROMETEO/2010/046 and ISIC/2012/009 to A. Ferrer-Montiel. L. Gregorio-Teruel has been a recipient of a fellowship from the Instituto Carlos III.

The authors declare no competing financial interests.

Sharona E Gordon served as editor.

Submitted: 25 July 2013
Accepted: 29 January 2014

## REFERENCES

Bhave, G., H.J. Hu, K.S. Glauner, W. Zhu, H. Wang, D.J. Brasier, G.S. Oxford, and R.W. Gereau IV. 2003. Protein kinase C phosphorylation sensitizes but does not activate the capsaicin receptor transient receptor potential vanilloid 1 (TRPV1). *Proc. Natl. Acad. Sci. USA.* 100:12480–12485. http://dx.doi.org/10.1073/pnas.2032100100

Brauchi, S., P. Orio, and R. Latorre. 2004. Clues to understanding cold sensation: thermodynamics and electrophysiological analysis of the cold receptor TRPM8. *Proc. Natl. Acad. Sci. USA.* 101:15494–15499. http://dx.doi.org/10.1073/pnas.0406773101

Brauchi, S., G. Orta, M. Salazar, E. Rosenmann, and R. Latorre. 2006. A hot-sensing cold receptor: C-terminal domain determines thermosensation in transient receptor potential channels. *J. Neurosci.* 26:4835–4840. http://dx.doi.org/10.1523/JNEUROSCI.5080-05.2006

Brauchi, S., G. Orta, C. Mascayano, M. Salazar, N. Raddatz, H. Urbina, E. Rosenmann, F. Gonzalez-Nilo, and R. Latorre. 2007. Dissection of the components for PIP2 activation and thermosensation in TRP channels. *Proc. Natl. Acad. Sci. USA.* 104:10246–10251. http://dx.doi.org/10.1073/pnas.0703420104

Cao, E., M. Liao, Y. Cheng, and D. Julius. 2013. TRPV1 structures in distinct conformations reveal activation mechanisms. *Nature.* 504:113–118. http://dx.doi.org/10.1038/nature12823

Caterina, M.J., and D. Julius. 2001. The vanilloid receptor: a molecular gateway to the pain pathway. *Annu. Rev. Neurosci.* 24:487–517. http://dx.doi.org/10.1146/annurev.neuro.24.1.487

Chowdhury, S., and B. Chanda. 2013. Free-energy relationships in ion channels activated by voltage and ligand. *J. Gen. Physiol.* 141:11–28. http://dx.doi.org/10.1085/jgp.201210860

Clapham, D.E. 2003. TRP channels as cellular sensors. *Nature.* 426:517–524. http://dx.doi.org/10.1038/nature02196

Clapham, D.E., and C. Miller. 2011. A thermodynamic framework for understanding temperature sensing by transient receptor potential (TRP) channels. *Proc. Natl. Acad. Sci. USA.* 108:19492–19497. http://dx.doi.org/10.1073/pnas.1117485108

Cohen, D.M. 2006. Regulation of TRP channels by N-linked glycosylation. *Semin. Cell Dev. Biol.* 17:630–637. http://dx.doi.org/10.1016/j.semcdb.2006.11.007

Fernández-Ballester, G., and A. Ferrer-Montiel. 2008. Molecular modeling of the full-length human TRPV1 channel in closed and desensitized states. *J. Membr. Biol.* 223:161–172. http://dx.doi.org/10.1007/s00232-008-9123-7

García-Sanz, N., A. Fernández-Carvajal, C. Morenilla-Palao, R. Planells-Cases, E. Fajardo-Sánchez, G. Fernández-Ballester, and A. Ferrer-Montiel. 2004. Identification of a tetramerization

domain in the C terminus of the vanilloid receptor. *J. Neurosci.* 24:5307–5314. http://dx.doi.org/10.1523/JNEUROSCI.0202-04.2004

García-Sanz, N., P. Valente, A. Gomis, A. Fernández-Carvajal, G. Fernández-Ballester, F. Viana, C. Belmonte, and A. Ferrer-Montiel. 2007. A role of the transient receptor potential domain of vanilloid receptor I in channel gating. *J. Neurosci.* 27:11641–11650. http://dx.doi.org/10.1523/JNEUROSCI.2457-07.2007

Grandl, J., S.E. Kim, V. Uzzell, B. Bursulaya, M. Petrus, M. Bandell, and A. Patapoutian. 2010. Temperature-induced opening of TRPV1 ion channel is stabilized by the pore domain. *Nat. Neurosci.* 13:708–714. http://dx.doi.org/10.1038/nn.2552

Horrigan, F.T., and R.W. Aldrich. 2002. Coupling between voltage sensor activation, Ca2+ binding and channel opening in large conductance (BK) potassium channels. *J. Gen. Physiol.* 120:267–305. http://dx.doi.org/10.1085/jgp.20028605

Jara-Oseguera, A., and L.D. Islas. 2013. The role of allosteric coupling on thermal activation of thermo-TRP channels. *Biophys. J.* 104:2160–2169. http://dx.doi.org/10.1016/j.bpj.2013.03.055

Jung, J., J.S. Shin, S.Y. Lee, S.W. Hwang, J. Koo, H. Cho, and U. Oh. 2004. Phosphorylation of Vanilloid Receptor 1 by Ca2+/Calmodulin-Dependent Kinase II Regulates Its Vanilloid Binding. *J. Biol. Chem.* 279:7048–7054. http://dx.doi.org/10.1074/jbc.M311448200

Labro, A.J., A.L. Raes, A. Grottesi, D. Van Hoorick, M.S. Sansom, and D.J. Snyders. 2008. Kv Channel Gating Requires a Compatible S4-S5 Linker and Bottom Part of S6, Constrained by Non-interacting Residues. *J. Gen. Physiol.* 132:667–680. http://dx.doi.org/10.1085/jgp.200810048

Labro, A.J., I.R. Boulet, F.S. Choveau, E. Mayeur, T. Bruyns, G. Loussouarn, A.L. Raes, and D.J. Snyders. 2011. The S4-S5 linker of KCNQ1 channels forms a structural scaffold with the S6 segment controlling gate closure. *J. Biol. Chem.* 286:717–725. http://dx.doi.org/10.1074/jbc.M110.146977

Latorre, R., S. Brauchi, G. Orta, C. Zaelzer, and G. Vargas. 2007. ThermoTRP channels as modular proteins with allosteric gating. *Cell Calcium.* 42:427–438. http://dx.doi.org/10.1016/j.ceca.2007.04.004

Liao, M., E. Cao, D. Julius, and Y. Cheng. 2013. Structure of the TRPV1 ion channel determined by electron cryo-microscopy. *Nature.* 504:107–112. http://dx.doi.org/10.1038/nature12822

Lin, Z., Q. Chen, M. Lee, X. Cao, J. Zhang, D. Ma, L. Chen, X. Hu, H. Wang, X. Wang, et al. 2012. Exome sequencing reveals mutations in TRPV3 as a cause of Olmsted syndrome. *Am. J. Hum. Genet.* 90:558–564. http://dx.doi.org/10.1016/j.ajhg.2012.02.006

Mandadi, S., T. Tominaga, M. Numazaki, N. Murayama, N. Saito, P.J. Armati, B.D. Roufogalis, and M. Tominaga. 2006. Increased sensitivity of desensitized TRPV1 by PMA occurs through PKCepsilon-mediated phosphorylation at S800. *Pain.* 123:106–116. http://dx.doi.org/10.1016/j.pain.2006.02.016

Matta, J.A., and G.P. Ahern. 2007. Voltage is a partial activator of rat thermosensitive TRP channels. *J. Physiol.* 585:469–482. http://dx.doi.org/10.1113/jphysiol.2007.144287

Nilius, B., and G. Owsianik. 2011. The transient receptor potential family of ion channels. *Genome Biol.* 12:218. http://dx.doi.org/10.1186/gb-2011-12-3-218

Nilius, B., K. Talavera, G. Owsianik, J. Prenen, G. Droogmans, and T. Voets. 2005. Gating of TRP channels: a voltage connection? *J. Physiol.* 567:35–44. http://dx.doi.org/10.1113/jphysiol.2005.088377

Pingle, S.C., J.A. Matta, and G.P. Ahern. 2007. Capsaicin receptor: TRPV1 a promiscuous TRP channel. *Handbook Exp. Pharmacol.* 179:155–171. http://dx.doi.org/10.1007/978-3-540-34891-7_9

Premkumar, L.S., and G.P. Ahern. 2000. Induction of vanilloid receptor channel activity by protein kinase C. *Nature.* 408:985–990. http://dx.doi.org/10.1038/35050121

Studer, M., and P.A. McNaughton. 2010. Modulation of single-channel properties of TRPV1 by phosphorylation. *J. Physiol.* 588:3743–3756. http://dx.doi.org/10.1113/jphysiol.2010.190611

Ufret-Vincenty, C.A., R.M. Klein, L. Hua, J. Angueyra, and S.E. Gordon. 2011. Localization of the PIP2 sensor of TRPV1 ion channels. *J. Biol. Chem.* 286:9688–9698. http://dx.doi.org/10.1074/jbc.M110.192526

Valente, P., N. García-Sanz, A. Gomis, A. Fernández-Carvajal, G. Fernández-Ballester, F. Viana, C. Belmonte, and A. Ferrer-Montiel. 2008. Identification of molecular determinants of channel gating in the transient receptor potential box of vanilloid receptor I. *FASEB J.* 22:3298–3309. http://dx.doi.org/10.1096/fj.08-107425

Valente, P., A. Fernández-Carvajal, M. Camprubí-Robles, A. Gomis, S. Quirce, F. Viana, G. Fernández-Ballester, J.M. González-Ros, C. Belmonte, R. Planells-Cases, and A. Ferrer-Montiel. 2011. Membrane-tethered peptides patterned after the TRP domain (TRPducins) selectively inhibit TRPV1 channel activity. *FASEB J.* 25:1628–1640. http://dx.doi.org/10.1096/fj.10-174433

Venkatachalam, K., and C. Montell. 2007. TRP channels. *Annu. Rev. Biochem.* 76:387–417. http://dx.doi.org/10.1146/annurev.biochem.75.103004.142819

Voets, T. 2012. Quantifying and modeling the temperature-dependent gating of TRP channels. *Rev. Physiol. Biochem. Pharmacol.* 162:91–119.

Voets, T., G. Droogmans, U. Wissenbach, A. Janssens, V. Flockerzi, and B. Nilius. 2004. The principle of temperature-dependent gating in cold- and heat-sensitive TRP channels. *Nature.* 430:748–754. http://dx.doi.org/10.1038/nature02732

Winter, Z., A. Buhala, F. Ötvös, K. Jósvay, C. Vizler, G. Dombi, G. Szakonyi, and Z. Oláh. 2013. Functionally important amino acid residues in the transient receptor potential vanilloid 1 (TRPV1) ion channel—an overview of the current mutational data. *Mol. Pain.* 9:30. http://dx.doi.org/10.1186/1744-8069-9-30

Wirkner, K., H. Hognestad, R. Jahnel, F. Hucho, and P. Illes. 2005. Characterization of rat transient receptor potential vanilloid 1 receptors lacking the N-glycosylation site N604. *Neuroreport.* 16:997–1001. http://dx.doi.org/10.1097/00001756-200506210-00023

Wu, Y., Y. Xiong, S. Wang, H. Yi, H. Li, N. Pan, F.T. Horrigan, Y. Wu, and J. Ding. 2009. Intersubunit coupling in the pore of BK channels. *J. Biol. Chem.* 284:23353–23363. http://dx.doi.org/10.1074/jbc.M109.027789

Yang, F., Y. Cui, K. Wang, and J. Zheng. 2010. Thermosensitive TRP channel pore turret is part of the temperature activation pathway. *Proc. Natl. Acad. Sci. USA.* 107:7083–7088. http://dx.doi.org/10.1073/pnas.1000357107

Yao, J., B. Liu, and F. Qin. 2010a. Kinetic and energetic analysis of thermally activated TRPV1 channels. *Biophys. J.* 99:1743–1753. http://dx.doi.org/10.1016/j.bpj.2010.07.022

Yao, J., B. Liu, and F. Qin. 2010b. Pore turret of thermal TRP channels is not essential for temperature sensing. *Proc. Natl. Acad. Sci. USA.* 107:E125. http://dx.doi.org/10.1073/pnas.1008272107